ELSEVIER

Polymer 41 (2000) 4719–4727

polymer

Crystal structures of α and β forms of poly(tetramethylene succinate)

Y. Ichikawa[a,1,2,*], H. Kondo[a], Y. Igarashi[a], K. Noguchi[a], K. Okuyama[a], J. Washiyama[b]

[a]*Faculty of Technology, Tokyo University of Agriculture and Technology, Koganei, Tokyo 184-8588, Japan*
[b]*Japan Polyolefins Co. Ltd, Kawasaki Development Center, 2-3-2, Yako, Kawasaki-ku, Kawasaki 210-3584, Japan*

Received 12 July 1999; received in revised form 9 September 1999; accepted 13 September 1999

Abstract

Crystal structures of the α and β modifications of poly(tetramethylene succinate) (PTMS) were analyzed by X-ray diffraction: the β form appeared with an application of stress. These two modifications belonged to the monoclinic system with the space group of $P2_1/n$. In both cases, a unit cell included two chemical repeating units. For the α form, the cell dimensions were $a = 0.523$ nm, $b = 0.912$ nm, c (fiber axis)$= 1.090$ nm, and $\beta = 123.9°$; for the β form, $a = 0.584$ nm, $b = 0.832$ nm, c (fiber axis)$= 1.186$ nm, and $\beta = 131.6°$. The difference in the fiber periods of the two crystalline forms was attributed mainly to the conformational difference in the tetramethylene unit, i.e. $TGT\bar{G}T$ of the α form and *TTTTT* of the β form. It was also found that in PTMS, the packing coefficient, *K*, which was defined by the ratio of the intrinsic volume with respect to the true volume of the α form was almost equal to that of the β form. This observation could be contrasted to those obtained in poly(butylene terephthalate) (PBT), where the *K* of the α form was considerably greater than that of the β form. The difference between PTMS and PBT was attributed to the difference between the unit cell volumes of the α and β forms of these polymers.

Keywords: Crystal structure; Biodegradable polymer; Poly(tetramethylene succinate)

1. Introduction

Biodegradable aliphatic polyesters have received much attention from industry, particularly from the ecological viewpoint [1]. Mechanical properties of such crystalline polymers depend strongly on their crystal structures, which could be changed by pressure, temperature and strain, as well as on the crystallinity of the polymers [2]. Recently, we have discovered crystal modifications (α and β forms) in poly(tetramethylene succinate) (PTMS). The transition occurred reversibly under the application and removal of strain: the β form appeared under strain [3]. The conformations of the two forms were reported to be ($T_7GT\bar{G}$) [4] and (T_{10}) [3] for the α and β forms, respectively, where *T*, *G* and $\bar{G}$ denoted *trans*, *gauche* and *minus gauche*, respectively. In this case, the conformation change occurred in the tetramethylene units [3]. In addition, the crystal transition mechanisms were investigated in detail by the authors [5].

The crystal structure analyses of several aliphatic polyesters, particularly those with an ethylene glycol unit, have been conducted [6–9]. In addition, the crystal structure of poly(trimethylene sebacate) was recently investigated by Jourdan et al. [10]. Despite many investigations on the crystal structure of ethylene series of aliphatic polyester, few works were reported on the tetramethylene series; the crystal structures of the α form in a uniaxially oriented fiber [4] and in a single crystal [11] were reported only in PTMS. However, no detailed crystal structures were presented in both cases.

Crystal transitions induced by strain (or stress) have been discovered in many polymers, and their crystal structure analyses were conducted [12–17]. However, most of them showed irreversible transitions [15–17]. For a reversible system, crystal structure analyses were conducted only in poly(butylene terephthalate) [PBT] [12,13] and PEO [14]. In PBT, for instance, two kinds of crystal modifications (α and β forms) were reported [12,13]: the β form appeared under strain. Yokouchi et al. [12] reported that the space groups of both α and β forms were $P\bar{1}$, and that their conformations in the tetramethylene units were $\bar{G}\bar{G}TGG$ (α form) and $T\bar{S}TST$ (β form), where *S* and $\bar{S}$ denoted *skew* and *minus skew*, respectively. At the same time, Hall et al. [13] reported that the space groups of these two forms were $P\bar{1}$, while the conformation of the β form to be *TTTTT*.

* Corresponding author. Tel.: +81-44-277-7186; fax: +81-44-299-2763.
E-mail address: ichikawa@kpl.sdk.co.jp (Y. Ichikawa).
[1] Present address: Kawasaki Plastics Laboratory, Showa Denko K.K., 3-2, Chidori-cho, Kawasaki-ku, Kawasaki 210-0865, Japan.
[2] On leave from Showa Denko K.K. Kawasaki Plastics Laboratory.

0032-3861/00/$ - see front matter
PII: S0032-3861(99)00659-X

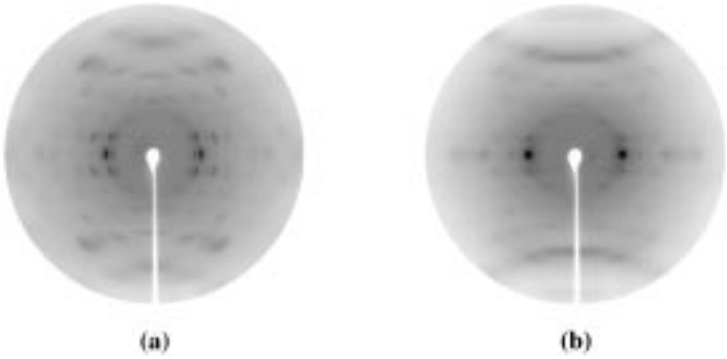

Fig. 1. Fiber diffraction patterns of (a) α and (b) β forms of poly(tetramethylene succinate).

In this paper, the crystal structures of both the α and β forms of PTMS were analyzed by the X-ray diffraction method.

2. Experimental section

2.1. Materials

The polymer material used in this study was poly(tetramethylene succinate) (PTMS), so called Bionolle, which was supplied from Showa Highpolymer Co. Ltd. No further purification was applied. The weight average molecular weight was determined to be 1.6×10^5 by size exclusion chromatography with poly(methylmethacrylate) standards. The melting (T_m) and glass transition temperatures (T_g) were measured by DSC and found to be 114 and −32°C, respectively. Further information can be seen elsewhere [3].

2.2. Sample preparation

Uniaxially oriented fibers were prepared by melt spinning at 200°C, followed by the drawing up to 10 times at room temperature, which were then annealed at 80°C in vacuum under a constant length. The diameter of the fibers was 500 μm. These fiber specimens were utilized in the following X-ray studies.

2.3. X-ray measurements

Most of the diffraction patterns were recorded on an imaging plate. A cylindrical camera with multiple X-ray film method was used in order to record reflections at higher angles as much as possible.

In the imaging plate method, a rotating-anode X-ray generator (RU-200, Rigaku) was operated in a normal focus mode to provide a monochromatized CuK_α beam (wave length $\lambda = 0.15418$ nm at 50 kV × 140 mA). Diffraction data were recorded on a disk-shaped imaging plate with the sample-plate distance of 75.5 mm. The diffraction pattern was read by measuring the fluorescence intensity stimulated by a focused He–Ne laser beam that scanned spirally on the surface of the imaging plate. The measurement of X-ray diffraction data was implemented by the hardware system, DIP100S (MAC Science). The intensity values were thereby converted into pixel data in a rectangular coordinate system. A whole area of the imaging plate (diameter ~200 mm) was divided into 1600×1600 pixels, each having a size of 125 mm^2. The correction of the background intensity was made separately for each diffraction spot according to a conventional method, followed by the correction using the Lorentz-polarization factor [18].

In the multiple-film method, the Ni-filtered CuK_α radiation was used. The reflection intensities were recorded on a cylindrical camera of a diameter of 100 mm.

2.4. Structure analysis

The structure analysis was conducted using the linked-atom least-squares program (LALS) [19]. Molecular models and packing structures were obtained by minimizing the quantity, Ω, defined by Eq. (1).

$$\Omega = \sum W_m(|F_{m,o}| - k|F_{m,c}|)^2 + \sum \varepsilon_{i,j} + \sum \lambda_q G_q \qquad (1)$$

Table 1
Crystal data of the α and β forms of PTMS.

	α form	β form
Crystal system	Monoclinic	Monoclinic
Space group	$P2_{1/n}$	$P2_{1/n}$
Cell dimension		
a (nm)	0.523(2)	0.584(5)
b (nm)	0.912(3)	0.832(11)
c(fiber axis) (nm)	1.090(5)	1.186(7)
β (°)	123.9(2)	131.6(5)
Volume (V/nm^3)	0.4315(30)	0.4320(80)
Density (ρ_{obs}/gcm^{-3})	1.28	–
(ρ_{cal}/gcm^{-3})	1.33	1.32
Number of chains running through the unit cell	2	2
Number of reflections used in this study		
Observed reflections	73	43
Unobserved reflections	46	40

where $F_{m,o}$ and $F_{m,c}$ denoted the observed and calculated structure factors, respectively. The k was a scaling factor, and m counts over all independent reflections. In the present analysis, we took into account the unobserved reflections within the highest observed diffraction angle by assuming their intensities to be a half of the weakest observed intensity. The weight factor, w_m, was chosen to be $w_m = 1.0$ for all the observed reflections. For the unobserved reflections, on the other hand, $w_m = 1.0$ when $|F_{m,c}| \geq |F_{m,o}|$, while $w_m = 0$ when $|F_{m,c}| < |F_{m,o}|$. The second term in the right-hand side evaluated the non-bonded repulsive energy, εij, arising between the non-bonded atoms i and j. The third term involved a set of coordinate constraint equations, G_q, and Lagrange multipliers, λ_q : these constraints were used to preserve a continuity of chains during the refinement calculation.

3. Crystal structure analyses

3.1. The α form

3.1.1. Unit cell and space group

Fig. 1(a) shows the fiber diffraction pattern of the α form. The observed reflections can be indexed based on the monoclinic cell, the cell dimensions of which are summarized in Table 1. The space group is determined to be $P2_1/n$ from the systematic absence rule [20]. The reflections appear only for *h0l* ($h + l$: even), *h00* (h: even), *0k0* (k: even) and *00l* (l: even): we have confirmed these absence rule up to the fifth layer line. This space group has been reported also in a single crystal [11] and in a uniaxially oriented fiber [4]. In the second, the calculated density of the α form under the assumption of two chemical repeating units per unit cell is 1.33 g/cm^3, which is in good agreement with the observed density of 1.28 g/cm^3. Therefore, two kinds of inversion center in the PTMS chemical structure have to be located at the crystallographic inversion center.

3.1.2. Molecular models

Fig. 2 shows the atomic numbering of PTMS. Due to the two inversion centers in a chemical repeating unit, the internal rotation angles should be $\theta_5 = \theta_{10} = T$, $\theta_1 = -\theta_9$, $\theta_2 = -\theta_8$ and $\theta_4 = -\theta_6$. Tadokoro [21] and Yokouchi et al. [22] reported that almost all aliphatic polyesters have a conformation of $\theta_3 = -\theta_7 = T$. Furthermore, according to the Cambridge Structure Database, the θ_3 (and θ_7) was found to be 160–200° in 5656 (99.7%), and 170–190° in 5402 (95.2%) out of 5672 compounds containing *C–O–C(=O)–C* structure and having crystallographic discrepancy index (*R*-factor) ≤ 0.07. Thus the assumption of $\theta_3 = -\theta_7 = T$ seems to be reasonable. As a result, independent parameters were thus reduced to only three (θ_1, θ_2 and θ_4). The possible internal rotation angles of θ_1 and θ_4 are T, G and $\bar{G}$. Those of θ_2 are T, G, $\bar{G}$, S, and $\bar{S}$. The latter two conformations were observed in poly(ethylene adipate) [6] for the *C–C–O–C(=O)*. The number of combination for the molecular conformations is 45. Because of inversion centers of this molecule, the number of independent models are reduced to 23. After the internal rotation angles are adjusted so that the fiber period is 1.090 nm, only five

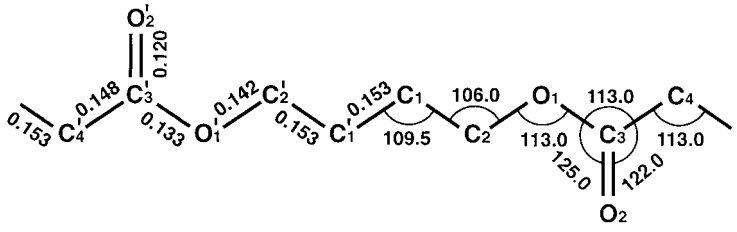

(a)

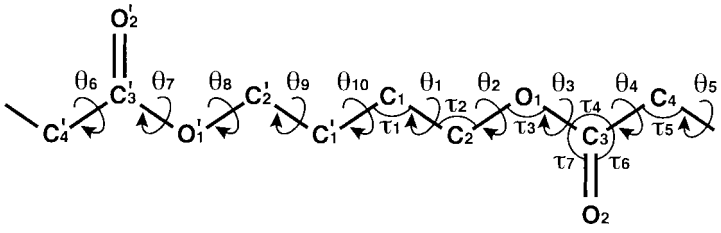

(b)

Fig. 2. (a) Atomic numbering scheme and standard bond lengths (nm) and angles (°) used in this study, together with (b) the definition of the bond angles and the internal rotation angles.

Table 2
Five plausible molecular models of the α form ($\theta_3 = -\theta_7 = T$, $\theta_5 = -\theta_{10} T$).

Model	A	B	C	D	E
$\theta_1(=-\theta_9)$	T	T	G	G	T
$\theta_2(=-\theta_8)$	$\bar{S}$	T	T	S	G
$\theta_4(=-\theta_6)$	$\bar{G}$	$\bar{G}$	T	T	$\bar{G}$

plausible molecular models (A–E) are conceivable (Table 2), while the other models are incompatible with this fiber period. In molecular model building, bond lengths and angles of poly(ethylene succinate) [9] (Fig. 2) are used.

3.1.3. Crystal structure

At first, two-dimensional (2D) (*c*-projection) analyses for the above five models were performed by using nine observed and five unobserved equatorial spots. The location of molecules in the unit cell can be uniquely obtained, since the center of symmetry in the chemical repeating unit must coincide with that in the unit cell. Therefore, the packing parameter is only the azimuthal angle of the molecules, which was surveyed by stepwise rotation of models around the molecular axis. In this study, evaluation of the packing structure was done by *R*-factors defined in Eqs. (2) and (3).

$$R = \left[\sum W_m(|F_{m,o}| - |F_{m,c}|)/\sum W_m F_{m,o}\right] \quad (2)$$

$$R_w = \left[\sum W_m(|F_{m,o}| - |F_{m,c}|)^2/\sum W_m F_{m,o}^2\right]^{1/2} \quad (3)$$

The two models [Model C($GT_7\bar{G}T$) and Model D ($GST_5\bar{S}\bar{G}T$)] showed better *R*-factors (0.22 and 0.20, respectively) compared with the remainders ($R > 0.3$). These two models were then analyzed using three-dimensional (3D) X-ray data (73 observed and 46 unobserved spots). The internal rotation angles and bond angles, together with an azimuthal angle, a scale factor and an attenuation factor were optimized, simultaneously. After

Table 3
Final refinement parameters of the α and β forms of PTMS.

		α form	β form
Torsional angle (°)	θ_1	62.9	180.0
	θ_2	−177.1	155.0
	θ_3	−178.7	178.8
	θ_4	−172.4	177.4
Bond angle (°)	τ_1	114.7	108.4
	τ_2	106.2	102.4
	τ_3	109.9	116.6
	τ_4	110.9	113.6
	τ_5	111.6	114.6
	τ_6	124.3	122.0
	τ_7	124.8	124.4
Scale factor		1.11	0.96
Attenuation factor		7.14	12.14
Eulerian angle (°)	ε_x	−115.26	−75.41
	ε_y	−62.08	−59.45
	ε_z	15.76	18.73
Azimuthal angle (°)	μ	−17.5	56.3
R-factor	*R*	0.19	0.14
	Rw	0.18	0.12
	R(ex)[a]	0.18	0.12
	Rw(ex)[a]	0.17	0.11

[a] *R*-factor was calculated excluding unobserved reflections.

Table 4
The final fractional atomic coordinates of the α and β forms of PTMS.

Atom	α form			β form		
	x	*y*	*z*	*x*	*y*	*z*
C_1	0.0839	0.0711	0.5389	0.0401	0.0372	0.5700
C_2	−0.0117	0.1387	0.6360	0.0049	0.0916	0.6496
C_3	−0.0195	0.0832	0.8352	−0.0286	0.0630	0.8347
C_4	0.0690	−0.0216	0.9564	0.0697	0.0284	0.9670
O_1	0.0696	0.0351	0.7495	0.0852	0.0075	0.7753
O_2	−0.1536	0.1964	0.8164	−0.1948	0.1766	0.7837
H_1a	0.0392	0.1534	0.4566	0.1116	0.1372	0.5383
H_1b	0.3308	0.0504	0.6104	0.2728	0.0802	0.6803
H_2a	0.1104	0.2419	0.6821	0.1563	0.1914	0.6803
H_2b	−0.2591	0.1590	0.5696	0.2280	0.1343	0.5754
H_4a	0.3190	−0.0237	1.0322	0.0077	0.1541	0.9370
H_4b	−0.0138	−0.1308	0.9106	0.3143	0.0186	1.0552

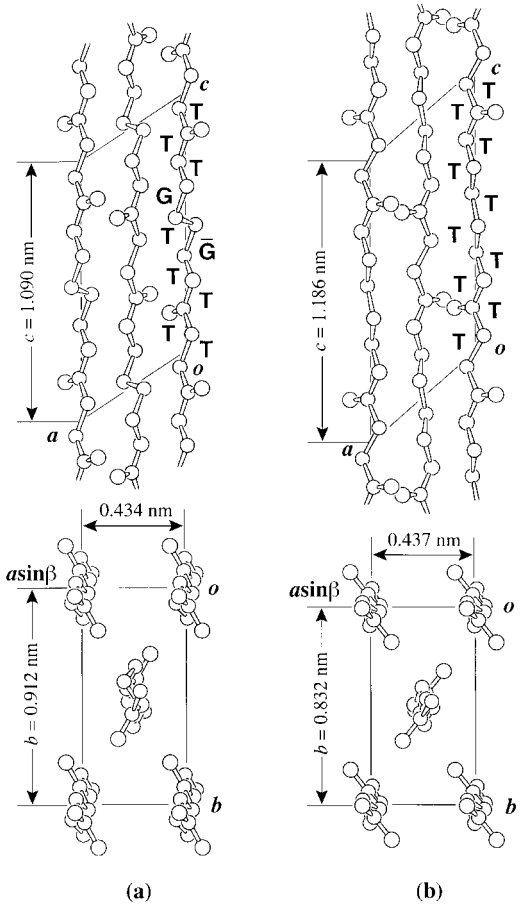

Fig. 3. Crystal structures of PTMS on the a'–b (bottom) and b–c (top) base planes are shown: (a) for the α form; (b) for the β form. All hydrogen atoms are omitted.

Table 5
Observed (F_o) and calculated (F_c) structure factors of the α form (reflections with F_o values in parentheses are those for unobserved reflections; these values are half of the observational threshold).

h	k	l	F_c	F_o
0	2	0	53.6	53.8
1	1	0	159.2	152.5
1	2	0	12.5	19.1
1	3	0	3.2	(4.9)
0	4	0	7.2	13.2
2	0	0	44.8	41.5
2	1	0		
1	4	0	48.2	45.0
2	2	0		
2	3	0	20.0	26.9
1	5	0	5.0	(6.2)
2	4	0	5.7	(6.5)
0	6	0	3.3	(6.6)
1	6	0	17.3	12.8
3	1	0		
2	5	0		
3	2	0		
3	3	0	5.7	(7.3)
1	7	0	8.6	11.2
2	6	0		
3	4	0		
0	1	1	6.8	9.0
−1	0	1	9.0	5.1
−1	1	1	34.0	38.1
0	2	1	73.8	73.0
−1	2	1	23.4	22.8
1	0	1	2.7	12.5
1	1	1	54.4	52.2
0	3	1	17.0	14.8
1	2	1	38.3	41.8
−1	3	1		
−2	1	1	8.9	12.0
1	3	1	26.1	28.7
0	4	1		
−2	2	1		
−1	4	1	8.9	16.7
−2	3	1	23.1	27.0
1	4	1		
2	1	1		
0	5	1	25.9	23.4
2	2	1		
−1	5	1		
−2	4	1	9.6	(6.2)
2	3	1	29.0	25.1
1	5	1		
−3	0	1		
−3	1	1		
0	6	1	14.1	16.9
−3	2	1		
−2	5	1	14.8	11.4
−1	6	1		
2	4	1		
−3	3	1	4.3	(6.9)
1	6	1	0.8	(7.0)
3	0	1	2.4	(7.2)
2	5	1	0.9	(7.3)
3	1	1	1.9	(7.3)
−3	4	1	3.7	(7.3)
−2	6	1	12.3	13.7
0	7	1		

Table 5 (*continued*)

h	k	l	F_c	F_o
3	2	1		
−1	7	1		
0	0	2	16.2	17.5
−1	1	2	2.9	8.8
0	1	2		
−1	2	2	15.7	15.9
0	2	2		
−2	0	2	9.2	11.4
−1	3	2	16.8	13.8
0	3	2		
−2	1	2		
1	1	2	16.1	18.0
−2	2	2	24.0	27.0
1	2	2	9.6	7.2
−1	4	2	15.6	11.6
0	4	2		
−2	3	2	9.1	9.8
1	3	2		
−2	4	2	7.8	14.5
−1	5	2		
0	5	2		
1	4	2		
−3	1	2	14.5	13.1
2	0	2		
2	1	2		
−3	2	2	5.5	(6.3)
2	2	2	2.2	(6.4)
−2	5	2	0.7	(6.5)
1	5	2	12.6	13.5
−3	3	2		
−1	6	2		
2	3	2		
0	6	2		
−1	1	3	16.2	23.3
0	1	3	13.2	18.7
−1	2	3		
0	2	3	2.1	9.8
−2	1	3		
−1	3	3	19.6	28.2
−2	2	3	2.8	(4.6)
0	3	3	15.9	13.4
1	0	3	7.4	16.6
1	1	3	14.7	16.8
−2	3	3		
−1	4	3		
1	2	3	2.0	(5.4)
0	4	3	4.4	11.7
−3	0	3	26.7	31.4
−3	1	3		
−2	4	3		
1	3	3		
−1	5	3	16.1	19.6
−3	2	3		
0	5	3	0.9	(6.1)
−3	3	3	11.8	8.9
1	4	3		
−2	5	3		
2	1	3	1.0	(6.6)
−1	6	3	15.8	11.9
−3	4	3		
2	2	3		
0	6	3		
1	5	3		

Table 5 (*continued*)

h	*k*	*l*	F_c	F_o
−2	6	3	2.6	(7.0)
2	3	3	5.5	(7.1)
−4	1	3	2.9	(7.2)
−3	5	3	4.7	(7.2)
−4	2	3	1.9	(7.4)
−1	7	3	5.8	(7.4)
1	6	3	13.1	17.9
2	4	3		
0	7	3		
−2	0	4	23.4	29.8
−1	2	4		
−2	1	4	13.7	(3.7)
0	0	4	7.8	(3.8)
0	1	4	26.8	26.4
−2	2	4	24.5	23.7
−1	3	4	47.8	54.3
0	2	4		
−2	3	4	2.6	(4.9)
0	3	4	10.4	12.8
−1	4	4	9.4	12.5
−3	1	4		
−2	4	4	25.0	15.1
1	1	4		
−3	2	4		
0	4	4		
1	2	4	15.3	14.7
−1	5	4	2.2	(5.9)
−3	3	4	4.4	(6.0)
1	3	4	10.9	14.5
−2	5	4		
0	5	4		
−3	4	4	3.7	(6.5)
1	4	4	8.9	11.2
−1	6	4		
−4	0	4	4.1	(6.8)
−4	1	4	6.4	(6.8)
−2	6	4	4.5	(6.9)
0	6	4	0.9	(7.0)
−3	5	4	0.2	(7.0)
2	0	4	4.7	(7.0)
−4	2	4	6.8	10.1
2	1	4	2.1	(7.1)
1	5	4	10.4	(7.1)
2	2	4	1.2	(7.2)
−4	3	4	2.7	(7.3)
−1	7	4	1.1	(7.4)
2	3	4	8.0	(7.5)
−3	6	4	9.4	14.5
−2	7	4		
−4	4	4		
0	7	4		
1	6	4		
−1	2	5	13.2	18.5
−2	2	5	23.3	25.1
0	1	5	11.2	6.3
−1	3	5		
−2	3	5	26.4	16.4
0	2	5		
−3	0	5		
−3	1	5	7.8	(4.9)
−3	2	5	14.4	11.1
−1	4	5		
0	3	5		

Table 5 (*continued*)

h	*k*	*l*	F_c	F_o
−2	4	5	6.8	(5.4)
−3	3	5	11.0	8.0
0	4	5	15.2	12.6
1	0	5		
1	1	5		
−1	5	5	9.1	(6.0)
−2	5	5	12.2	14.1
1	2	5		
−3	4	5		

refinement, model C showed $R = 0.19$, $Rw = 0.18$ and $\Omega = 1.71 \times 10^3$. On the other hand, model D showed $R = 0.24$, $Rw = 0.22$ and $\Omega = 2.50 \times 10^3$. In addition, no short contact is observed in model C [the shortest interatomic distance was 0.260 nm (between H_7b band O_4)]. While, short atomic contacts were found in model D [the shortest interatomic distance was 0.199 nm (between H_7b band O_4)]. These results indicate that model C is more preferable. The finally refined parameters are summarized in Table 3. The final fractional atomic coordinates are listed in Table 4, and the packing structures are shown in Fig. 3(a). The observed and calculated intensities are given in Table 5.

3.2. The β form

3.2.1. Unit cell

The observed spots in the fiber diffraction pattern of the β form (Fig. 1(b)), can be indexed by a monoclinic system (*b*-unique) similar to the α form. The cell dimensions are given in Table 1. Since the β form is stable only under tension, it is difficult to measure its density. Since the unit cell volume of the β form is almost equal to that of the α form, the number of chemical repeating unit was assumed to be same as that in the α form. With this assumption, the density was calculated to be 1.32 g/cm^3.

3.2.2. Space group

Since the number of observed spots was not enough to apply the systematic absence rule, the space group could not be determined unequivocally. Therefore, at first, the plane group (*c*-projection structure) was determined using equatorial reflections among all the monoclinic plane groups. The candidates of the plane group are *pm*, *pg*, *cm*, *p2mm*, *p2mg*, *p2gg* and *c2mm* [20]. Both *cm* and *c2mm* were rejected in terms of the systematic absence rule. In the case of *p2mm*, the molecular chains must be located on a mirror plane, which yields a large steric hindrance. The *R*-factors of both *pm* and *p2mg* were found to be rather high ($R > 0.4$) compared with those of *pg* and *p2gg* ($R \sim 0.2$). It was also found that in the case of *pg*, the center of the molecular chain was located approximately 0.25*b* (*a*-glide) or 0.25*a* (*b*-glide) apart from its respective glide

Table 6
Observed (F_o) and calculated (F_c) structure factors of the β form (reflections with F_o values in parentheses are those for unobserved reflections; these values are half of the observational threshold).

h	k	l	F_c	F_o
0	2	0	79.9	78.2
1	1	0	158.1	161.5
1	2	0	36.8	34.6
1	3	0	33.5	35.9
2	0	0	26.1	25.3
2	1	0	17.7	12.6
0	4	0		
2	2	0	39.6	35.1
1	4	0	6.8	(6.1)
2	3	0	3.8	(6.5)
1	5	0	9.8	16.3
2	4	0		
0	1	1	9.3	10.1
−1	0	1	10.6	12.7
−1	1	1	20.3	26.0
0	2	1	49.2	40.1
−1	2	1	25.2	25.2
1	0	1		
1	1	1	24.4	24.2
0	3	1	8.9	(5.0)
1	2	1	31.4	27.8
−1	3	1		
−2	1	1		
−2	2	1	4.1	(5.6)
1	3	1	11.0	13.7
0	4	1	3.6	(5.9)
−1	4	1	4.9	(6.0)
−2	3	1	15.4	16.2
2	1	1	6.4	(6.3)
1	4	1	11.1	14.6
2	2	1		
−1	5	1	11.1	15.3
−2	4	1		
−1	1	2	27.4	27.1
0	0	2		
0	1	2	6.9	(4.2)
−1	2	2	13.9	15.8
0	2	2	7.8	12.2
−2	0	2	11.7	18.2
−2	1	2	0.8	(4.7)
−1	3	2	7.2	(5.0)
0	3	2	20.5	18.3
−2	2	2		
1	1	2		
1	2	2	7.0	(5.6)
−2	3	2	4.2	(5.8)
−1	4	2	9.3	11.7
0	4	2	0.1	(6.0)
1	3	2	4.6	(6.1)
−3	1	2	3.5	(6.3)
−2	4	2	3.4	(6.5)
−3	2	2	6.8	(6.6)
2	0	2	9.1	13.2
−1	5	2		
1	4	2		
−1	1	3	0.3	(2.8)
−1	2	3	11.8	12.8
0	1	3		
−2	1	3	0.2	(4.2)
−2	2	3	21.5	19.3
0	2	3		
−1	3	3	11.5	15.4
0	3	3	1.7	(5.5)
−2	3	3	1.8	(5.5)
1	0	3	9.4	12.8
−3	0	3		
−3	1	3	3.9	(5.8)
−1	4	3	0.3	(5.9)
1	2	3	14.1	13.9
0	4	3		
−3	2	3		
−2	4	3		
−1	1	4	2.4	(3.0)
−2	0	4	17.9	24.8
−2	1	4	4.5	(3.6)
−1	2	4	9.4	16.9
−2	2	4	20.2	19.3
0	0	4		
0	1	4	9.9	(4.7)
−1	3	4	23.1	21.1
0	2	4	2.9	(5.2)
−2	3	4	1.8	(5.3)
−3	1	4	5.5	(5.3)
−3	2	4	7.5	(5.7)
0	3	4	0.1	(5.8)
−1	4	4	6.3	(5.9)
−2	4	4	11.2	11.3
−2	1	5	8.8	(2.8)
−1	1	5	24.9	27.0
−2	2	5	31.9	33.0
−1	2	5	4.1	(4.3)
−3	0	5	18.2	20.6
−3	1	5	7.2	(4.8)
−2	3	5	23.4	16.7
0	1	5		
−1	3	5		
−3	2	5	6.1	(5.2)
0	2	5	6.9	(5.6)
−3	3	5	10.4	12.1
−2	2	6	15.8	16.7
−1	1	6		
−3	1	6		
−1	2	6	6.4	(4.6)
−3	2	6	4.6	(4.7)
−2	3	6	2.4	(4.9)
−1	3	6	10.5	16.1

plane, indicating that *pg* and *p2gg* were essentially the same. Therefore, the plane group *p2gg* is adopted. The space groups having the plane group of *p2gg* in a monoclinic system (*b*-unique) are $P2_1/n$ and $P2_1/a$ [20]. Since the (−101) reflection was observed, $P2_1/a$ is not suitable, where only (*h0l*) with $l =$ even reflections should be observed. The following analysis, therefore, was performed under the space group of $P2_1/n$.

3.2.3. Crystal structure

Since the observed fiber period ($c = 1.186$ nm) was close to that of the all-*trans* conformation model

(1.199 nm), this was assumed as the molecular conformation of the β form. The internal rotation angles were adjusted so as to reproduce the actual fiber period, together with reducing the *R*-factor. In this calculation, four torsional angles (θ_1, θ_2, θ_3 and θ_4), seven bond angles (τ_1, τ_2, τ_3, τ_4, τ_5, τ_6 and τ_7), one azimuthal angle, a scale factor and an attenuation factor were refined by using independent 43 observed and 40 unobserved reflection spots. The finally refined parameters and the fractional atomic coordinates are summarized in Tables 3 and 4, respectively. The crystal structure of the β form is shown in Fig. 3(b), where the conformation of the tetramethylene unit is *TTTTT* (155.0°, 180.0°, 180.0°, 180.0°, −155.0°). The comparison between the observed and calculated intensities is made in Table 6. The shortest distance between nonbonded atoms was 0.243 nm (between O_4 and H_6a), and no unallowable short contact was observed.

4. Discussion

4.1. Crystal structure of α form

Recently, Pazur et al. [23] proposed a molecular model of the α form of PTMS based on the energy calculation of a single chain. Their final molecular structure corresponded to the model B in the present study. This was, however, ruled out in the stage of the 2D analysis. Nevertheless, 3D refinement of the model B was performed for comparison. After several refinement cycles, the model B showed $R = 0.36$ and $Rw = 0.35$, which were considerably higher than those for the model C ($R = 0.19$ and $Rw = 0.18$). Therefore, the molecular model proposed by Pazur et al. was not suitable in terms of the X-ray data. In addition, some short contacts were observed (H_1b–H_7a, 0.187 nm and O_4–H_2a, 0.188 nm). So, the model B was rejected.

Although the present result seems to be substantially same as that reported by Chatani et al. [4], further confirmation of the molecular structure of PTMS is obtained as well as its detailed information about the crystal structure of the α form.

4.2. Molecular packing

It is noteworthy that the two crystal forms in PTMS have the same and relatively high symmetry of $P2_1/n$. Such conservation of the symmetry between α and β forms has been reported also in PBT [12,13], although the symmetry of them ($P\bar{1}$) is relatively low. As shown in Fig. 3, the molecular packing in PTMS of both α and β forms is similar to that in polyethylene (orthorhombic form) [24]. Such polyethylene-like molecular packing has been reported in several aliphatic polyesters; e.g. poly(ethylene adipate) [6], poly(ethylene sebacate) [6] and poly(ethylene suberate) [7,8].

The packing coefficient, *K*, defined by Eq. (4) was considered [12].

$$K = V_{int}/V_{true} \tag{4}$$

where V_{int} denotes the intrinsic volume and is calculated from the group contribution concept, and V_{true} corresponds to the true volume, which can be obtained from the density and molecular weight of a repeating unit [25]. In Table 7, the *K* of α and β forms of PTMS as well as PBT is summarized. In PTMS, the *K* of the α form ($K = 0.70$) is equal to that of the β form ($K = 0.70$). In the case of PTMS, the cross-sectional area normal to the *c*-axis decreases upon the crystal transition from α to β form. More precisely, the *b*-axis contracts and the length of the a'-axis ($a \sin \beta$) remains approximately constant, while the *c*-axis extends (Table 7). Such a decrease in the cross-sectional area can be allowed by no bulky group of PTMS[3]. As a result, volumes of both unit cells are very close to each other, resulting in the almost equal value of *K* for both the crystal forms.

Table 7
Packing coefficient of α and β forms in PTMS and PBT.

	PTMS		PBT	
	α form	β form	α form	β form
K	0.70	0.70	0.74	0.68
a' (nm)	0.434	0.437	0.437	0.421
b (b') (nm)	0.912	0.832	0.586	0.555
c (nm)	1.090	1.186	1.159	1.295
A[a] (nm^2)	0.396	0.364	0.227	0.214

[a] Cross-sectional area normal to the *c*-axis.

As opposed to the case of PTMS, the *K* of the α form ($K = 0.74$) is greater than that of the β form (0.68) in the case of PBT. In this case, the lengths of both a' and b' axes remain approximately constant before and after the crystal transition. The cross-sectional area of a single chain of PBT on the *c*-projection plane is dictated mainly by the bulky phenyl rings. The conformation change in the tetramethylene unit has thus little effect on the cross-sectional area of a single chain[4], which resulted in the approximately constant cross-section upon the transition. Therefore, the *c*-axis extension after transition caused a smaller number of *K* of the β form in PBT (see Table 7).

4.3. Conformation of the β form

The length of the *c*-axis of the β form is slightly shorter than that of the fully extended structure. This is due to the highly deviated θ_2 angle (−155.0°). Polyesters comprising ethylene glycol and diacid units have a conformation similar

[3] It should be pointed out that no specific interaction (e.g. hydrogen bonds), which may restrict the deformation of a unit cell, among chains in the case of PTMS is included.

[4] Indeed, an approximately constant number of K was reported, when the conformation of phenyl rings drastically changed: $K = 0.70$ for both the α [26] and β forms [15].

to planar zig-zag, but not fully extended, when the number of CH_2 in the acid unit is greater than or equals to four. Poly(ethylene adipate) [6] and poly(ethylene suberate) [7–9], however, contain a *S* conformation at the same position (at θ_2). These observations indicate that the distortion at θ_2 tends to easily take place in such aliphatic polyesters.

4.4. Tilting

The "tilting" was firstly reported by Daubeny [27] in PET, where the *c*-axis does not coincide with the drawing direction in uniaxially drawn specimens. The authors observed the tilting in the α form of PTMS, while no tilting was observed in the β form. The tilting angle around the *b*-axis was obtained to be 1.7° based on the method reported by Daubeny et al. [27], indicating the validity of the indexing of the reflections.

5. Conclusion

Structure analyses of the two crystal modifications (α and β) of PTMS ($[-O(CH_2)_4OCO(CH_2)_2CO-]_n$), were performed by X-ray diffraction. Both of the modifications belonged to the monoclinic system with the space group of $P2_1/n$. In both the cases, the unit cell contained two molecular chains; the cell dimensions were $a = 0.523$ nm, $b = 0.912$ nm, c (fiber axis) $= 1.090$ nm, and $\beta = 123.9°$ for the α form; $a = 0.584$ nm, $b = 0.832$ nm, c (fiber axis) $= 1.186$ nm, and $\beta = 131.6°$ for the β form. The molecular conformations of the α and β forms were $GT\bar{G}T_7$ and T_{10}, respectively.

In PTMS, the packing coefficient, *K*, which was defined by the ratio of the intrinsic volume with respect to the true volume of the crystal cell, of the α form ($K = 0.70$) was equal to that of the β form ($K = 0.70$) within the experimental error, while in PBT, the *K* of the α form ($K = 0.74$) was larger than that of the β form ($K = 0.68$). The difference arose from the change of the cross-section of $a' - b$ (for PTMS) or $a' - b'$ (for PBT) plane on the *c*-projection plane upon the transition. In the case of PTMS which has no bulky group, the cross-section decreased and the *c*-axis extended upon transition. On the other hand, in PBT case, the *c*-axis extended without any cross-section change, since the size of the cross-section was dictated by the bulky phenyl rings.

"Tilting" in the α form of PTMS was observed, while no tilting was observed in the β form. The tilting angle around the *b*-axis was found to be 1.7°.

Acknowledgements

The authors would like to acknowledge the fruitful and stimulus discussion with emeritus Professor Y. Chatani of Tokyo University of Agriculture and Technology. This research was partially supported by a Grant-in-aid for Scientific Research (09750984) from the Ministry of Education, Science, Sports and Culture of Japan.

References

[1] Doi Y, Fukuda K. Biodegradable plastics and polymers, Amsterdam: Elsevier, 1994. pp. 577–90.
[2] Nielsen LE. Mechanical properties of polymers and composites, New York: Marcel Dekker, 1975.
[3] Ichikawa Y, Suzuki J, Washiyama J, Moteki Y, Noguchi K, Okuyama K. Polymer 1994;35(15):3338–9.
[4] Chatani Y, Hasegawa R, Tadokoro H. Polym Prep Jpn 1971:420.
[5] Ichikawa Y, Washiyama J, Moteki Y, Noguchi K, Okuyama K. Polym J 1995;27(12):1230–8.
[6] Turner-Jones A, Bunn CW. Acta Crystallogr 1962;15:105–13.
[7] Kanamoto T, Tanaka K, Nagai H. J Polym Sci A-2 1971;9(11):2043–60.
[8] Hobbs SY, Billmeyer Jr. FW. J Polym Sci A-2 1969;7(6):1119–21.
[9] Ueda AS, Chatani Y, Tadokoro H. Polym J 1971;2(3):387–97.
[10] Jourdan N, Deguire S, Bisse F. Macromolecules 1995;28(7):8086–91.
[11] Ihn KJ, Yoo ES, Im SS. Macromolecules 1995;28(7):2460–4.
[12] Yokouchi M, Sakakibara Y, Chatani Y, Tadokoro H, Tanaka T, Yoda K. Macromolecules 1976;9(2):266–73.
[13] Hall IH, Pass MG. Polymer 1976;17(9):807–16.
[14] Takahashi Y, Sumita I, Tadokoro H. J Polym Sci Polym Phys Ed 1973;11:2113–22.
[15] Takahashi Y, Kurumizawa T, Kusanagi H, Tadokoro H. J Polym Sci Polym Phys Ed 1978;16:1989–2003.
[16] Miyasaka K, Ishikawa K. J Polym Sci A-2 1968;6(7):1317–29.
[17] Lando JB, Olf HG, Peterlin A. J Polym Sci A-1 1966;4:941–51.
[18] Okuyama K, Noguchi K, Miyazawa T, Yui T, Ogawa K. Macromolecules 1997;30(19):5849–55.
[19] Smith PJC, Arnott A. Acta Crystallogr 1972;A34(1):3–11.
[20] International tables for crystallography. A. Space-groups symmetry. In: Hahn T, editor. Dordrecht, Holland: Reidel, 1983.
[21] Tadokoro H. Structure of crystalline polymers, New York: Wiley, 1979 chap. 7.
[22] Yokouchi M, Chatani Y, Tadokoro H, Teranishi K, Tani H. Polymer 1973;14(6):267–72.
[23] Pazur RJ, Raymond S, Hocking PJ, Marchessault RH. Polymer 1998;39(14):3065–72.
[24] Bunn CW. Trans Faraday Soc 1939;35:482–91.
[25] Slonimskii GL, Askadskii AA, Kitaigorodskii AI. Vysokomol Soyed A 1970;12(3):494–512.
[26] Kusanagi H, Tadokoro H, Chatani Y, Suehiro K. Macromolecules 1977;10(2):405–13.
[27] Daubeny RP, Bunn CW, Brown CJ. Proc R Soc London A 1954;226:531–42.